Supplemental Material: Nonuniversality of Aging during Phase Separation of the Two-Dimensional Long-Range Ising Model

Fabio Müller,[1,*] Henrik Christiansen,[1,2,†] and Wolfhard Janke[1,‡]

[1]*Institut für Theoretische Physik, Universität Leipzig, IPF 231101, 04081 Leipzig, Germany*
[2]*NEC Laboratories Europe GmbH, Kurfürsten-Anlage 36, 69115 Heidelberg, Germany*
(Dated: September 12, 2024)

This Supplemental Material contains the raw data for the autocorrelation function. For these data the dynamical scaling for the two most common scaling variables $y = t/t_w$ and $x = \ell(t)/\ell(t_w)$ is presented. Additionally, details on the fitting procedure for the chosen scaling variable y are discussed, where in particular the choice of parameters of the fits and the resulting fitting parameters are presented. Finally, the influence of the inclusion of an asymptotic correction term into the fit ansatz is investigated.

LOSS OF TIME-TRANSLATION INVARIANCE AND DYNAMICAL SCALING

One main aspect of aging is the loss of time-translation invariance of the autocorrelation function $C(t, t_w)$, i.e., $C(t, t_w)$ shows no scaling as a function of $t - t_w$. Instead one observes dynamical scaling in terms of $y = t/t_w$ or $x = \ell(t)/\ell(t_w)$. For the scaling variable y, this is demonstrated in Fig. S1, where for all the considered values of σ and the nearest neighbor model (NN) the autocorrelation function $C(t, t_w)$ is shown for different waiting times. The main plots show $C(t, t_w)$ as a function of y and the insets show the same data as a function of $t - t_w$. The plots contain also data which is finite-size affected (see next section) for which deviations from the master curve are expected. For a facilitated distinction of the finite-size affected data, we have plotted the corresponding points transparently.

While clearly time-translation invariance is broken, as visible from the inset, the data collapse in the main plots is excellent for all σ and the NN model. The earliest waiting time was chosen in such a way that it is minimal but without affecting the quality of the dynamical scaling. For the fits in the next section, only the data for this earliest t_w is taken since it offers the longest period of finite-size unaffected data. The other waiting times were chosen in such a way that dynamical scaling is clearly visible.

Using the same values of t_w as in Fig. S1, the quality of the dynamical scaling for the variable x is investigated in Fig. S2, where another illustration of the broken time-translation invariance is not provided but the finite-size affected data are again plotted transparently. With an appropriate zoom into the figure, it is clearly visible, that the quality of the dynamical scaling for most values of σ is noticeably compromised. Due to the more consistent dynamical scaling in y we will only perform the fits using y as scaling variable.

FITTING PROCEDURE

Now that the prerequisites for aging are checked, the autocorrelation exponent can be extracted from the data. In the following, we present a detailed discussion of the fitting procedure for the two different ansätze where first a simple (asymptotic) power law

$$f(y) = Ay^{-\lambda/z} \tag{S.1}$$

is used. Additionally, an ansatz

$$f(y) = Ay^{-\lambda/z}(1 - B/y) \tag{S.2}$$

is considered which includes a low-order correction term, accounting for preasymptotic effects. The growth exponent z is always kept fixed to its theoretical value $z = \min(2+\sigma, 3)$. At the crossover point $\sigma = 1$ both the equilibrium critical behavior as well as the asymptotic growth of the characteristic length scale $\ell(t)$ carry logarithmic corrections. Since the autocorrelation function $C(t, t_w)$ for $\sigma = 1$ does not show any peculiarities indicating a possible logarithmic correction, however, we do not include any logarithmic correction term into the fitting ansatz for $\sigma = 1$ either.

As discussed in the main text, the fitting interval $[y_{\min}, y_{\max}]$ is chosen in the following way: First all data for which noticeable finite-size effects in $\ell(t)$ are visible (cf. Fig. 2 in the main text) are discarded. The $y_{\max}$ is determined roughly from the deviations of the autocorrelation functions for the chosen t_w and the next larger t_w. In some cases, however, the fluctuation of $C(t, t_w)$ are already quite strong, even for $y < y_{\max}$, in which cases we reduced the value of $y_{\max}$ further. This avoids an increase in statistical errors and the accumulation of systematic errors. The values of $y_{\min}$ were chosen in such a way that the fit interval is maximal with the restriction that no strong systematic trend in the resulting fit parameters is visible and the value of χ^2/dof does not show any strong increase. Note that the value of χ^2/dof has no absolute meaning since the data are correlated. However, a strong ramp remains an indication that the ansatz becomes inappropriate for the data. The above procedure is illustrated in Figs. S3 and S4 for the ansatz without and with correction term, respectively, showing the dependence of χ^2/dof and the fitting parameters on $y_{\min}$. Both ansätze show a sharp increase of χ^2/dof for decreasing $y_{\min}$, which is accompanied also by an onset of stronger trends in the resulting fit parameters. Especially for the fits including the correction term in Fig. S4, there are very pronounced plateaus in the resulting fit parameters which underscore the robustness of the ansatz. We have thus decided to present the values of λ obtained from the fits with the correction term in the main text, since they seem to be more robust and thus less prone to systematic errors.

The resulting fits, together with the fitted correlation function are presented in Fig. S5 and Fig. S6 without and with correction term, respectively. The fits with correction term describe the data over a significantly longer interval compared to the corresponding fit without correction, explaining the enhanced stability of the resulting fit parameters. In Tables S1 and S2 the input parameters for the fits and the parameters of the outcoming best fitting curves are reported for convenience such that the interested reader can better compare the different settings and results. Finally, the dependence of λ on σ is compared for the two ansätze in Fig. S7. There it is clearly visible that the fits with and without correction are for most values of σ in very good qualitative agreement. The statistical errors which we assess by Jackknifing over the different realizations (initial conditions and thermal noises) tend to be reduced upon introducing the correction term. While increased statistical errors would be expected due to the additional fitting parameter, the significantly extended fitting ranges overcompensate this effect, enabling a clear statement about the crossover behavior in the regime $1 \lesssim \sigma \lesssim 2$.

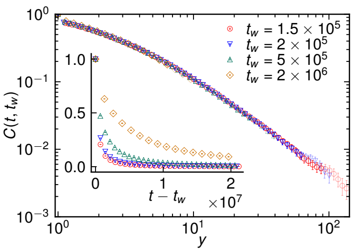

(a) $\sigma = 0.6$

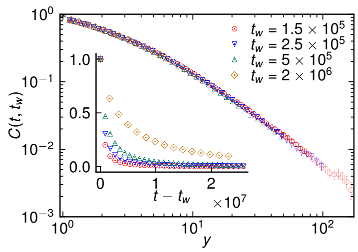

(b) $\sigma = 0.8$

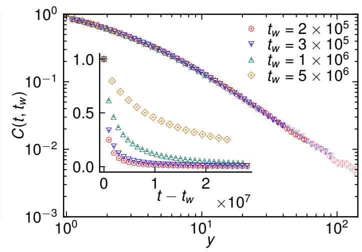

(c) $\sigma = 0.9$

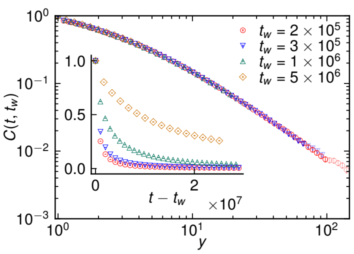

(d) $\sigma = 1$

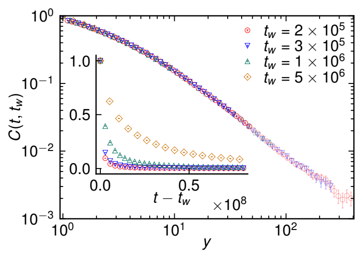

(e) $\sigma = 1.1$

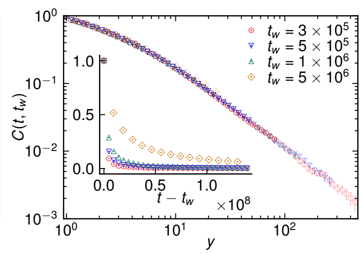

(f) $\sigma = 1.5$

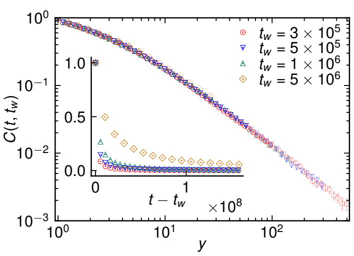

(g) $\sigma = 2$

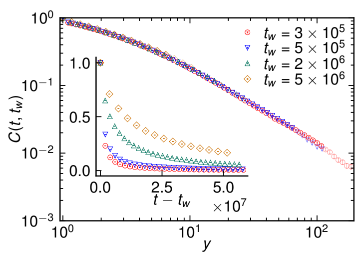

(h) $\sigma = 3$

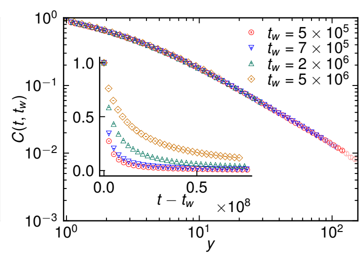

(i) $\sigma = 10$

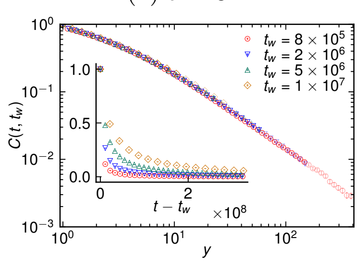

(j) NN

FIG. S1: Illustration of dynamical scaling with respect to $y = t/t_w$ (main plots) and loss of time-translation invariance (insets).

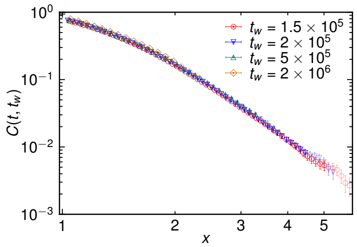

(a) $\sigma = 0.6$

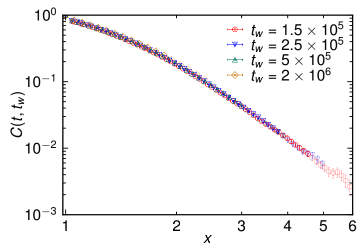

(b) $\sigma = 0.8$

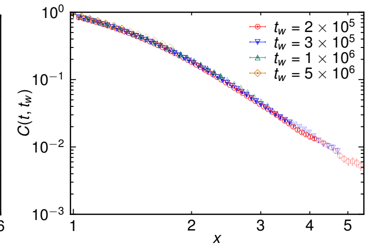

(c) $\sigma = 0.9$

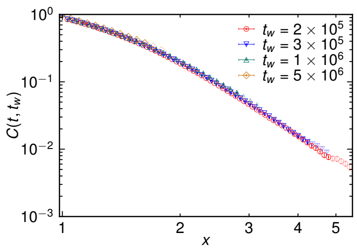

(d) $\sigma = 1$

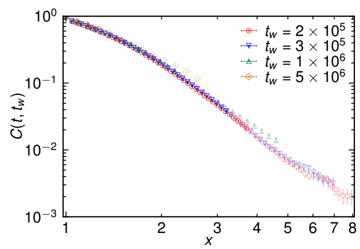

(e) $\sigma = 1.1$

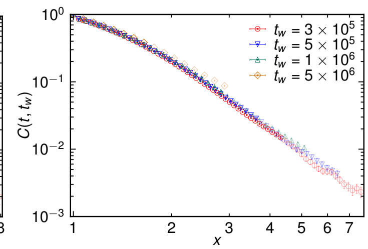

(f) $\sigma = 1.5$

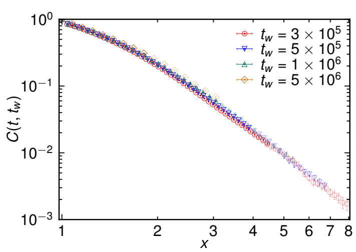

(g) $\sigma = 2$

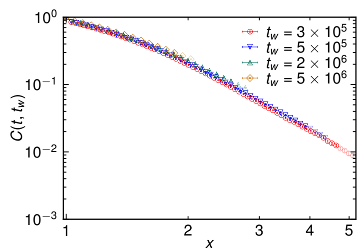

(h) $\sigma = 3$

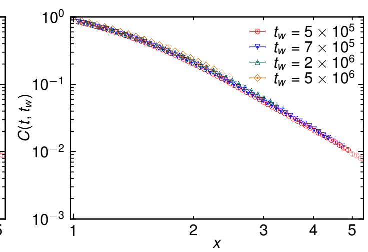

(i) $\sigma = 10$

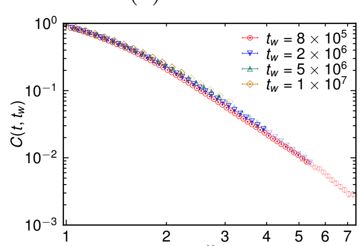

(j) NN

FIG. S2: Illustration of dynamical scaling with respect to $x = \ell(t)/\ell(t_w)$. For most σ the data collapse is considerably worse than for the scaling variable y used in Fig. S1.

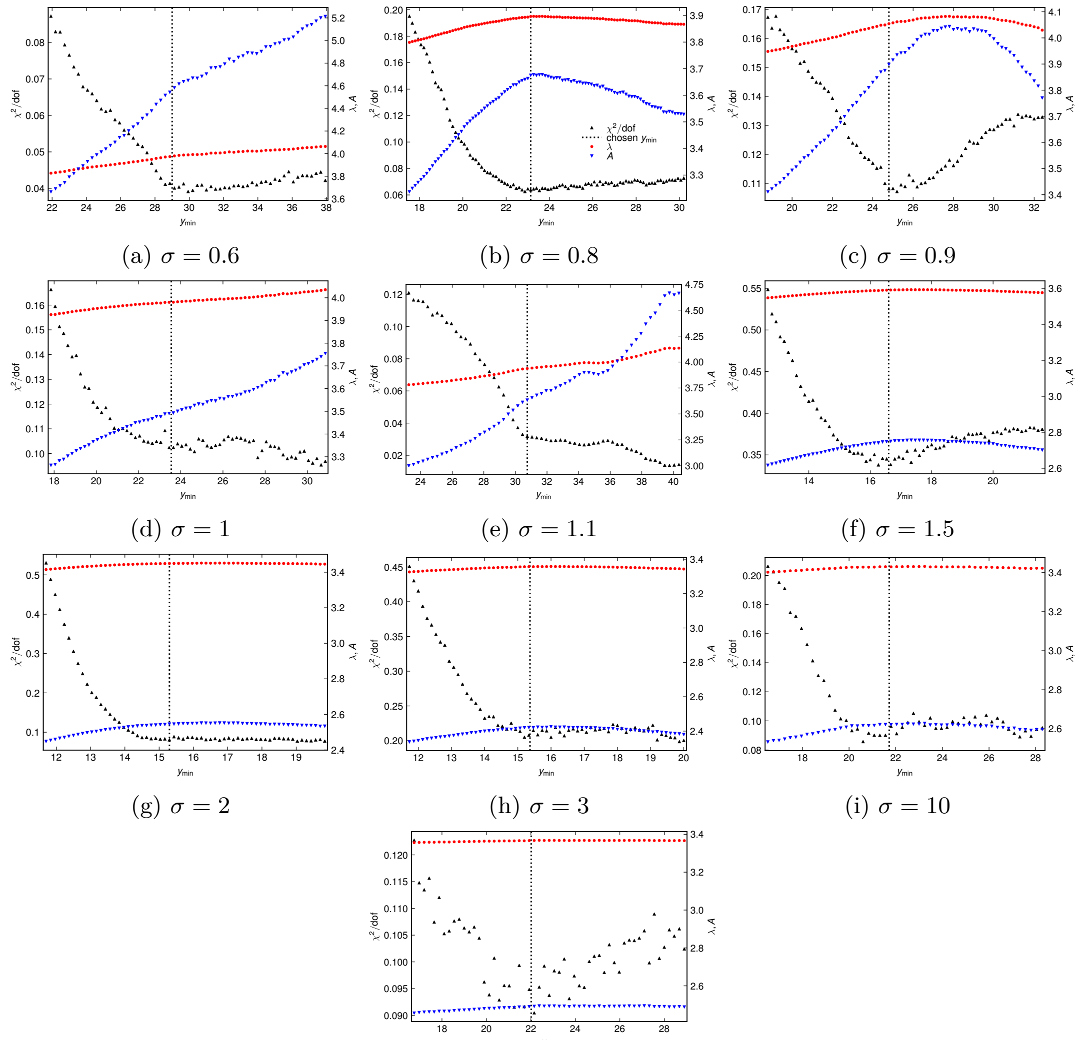

(a) $\sigma = 0.6$ (b) $\sigma = 0.8$ (c) $\sigma = 0.9$

(d) $\sigma = 1$ (e) $\sigma = 1.1$ (f) $\sigma = 1.5$

(g) $\sigma = 2$ (h) $\sigma = 3$ (i) $\sigma = 10$

(j) NN

FIG. S3: Illustration of the influence of the choice of the lower fit boundary $y_{\rm min}$ on $\chi^2/\rm dof$ and the resulting fit parameters for the asymptotic fit ansatz $f(y) = Ay^{-\lambda/z}$ with $y = t/t_w$ using the smallest t_w for each σ (cf. Fig. S1). The vertical dotted lines indicate the finally chosen $y_{\rm min}$.

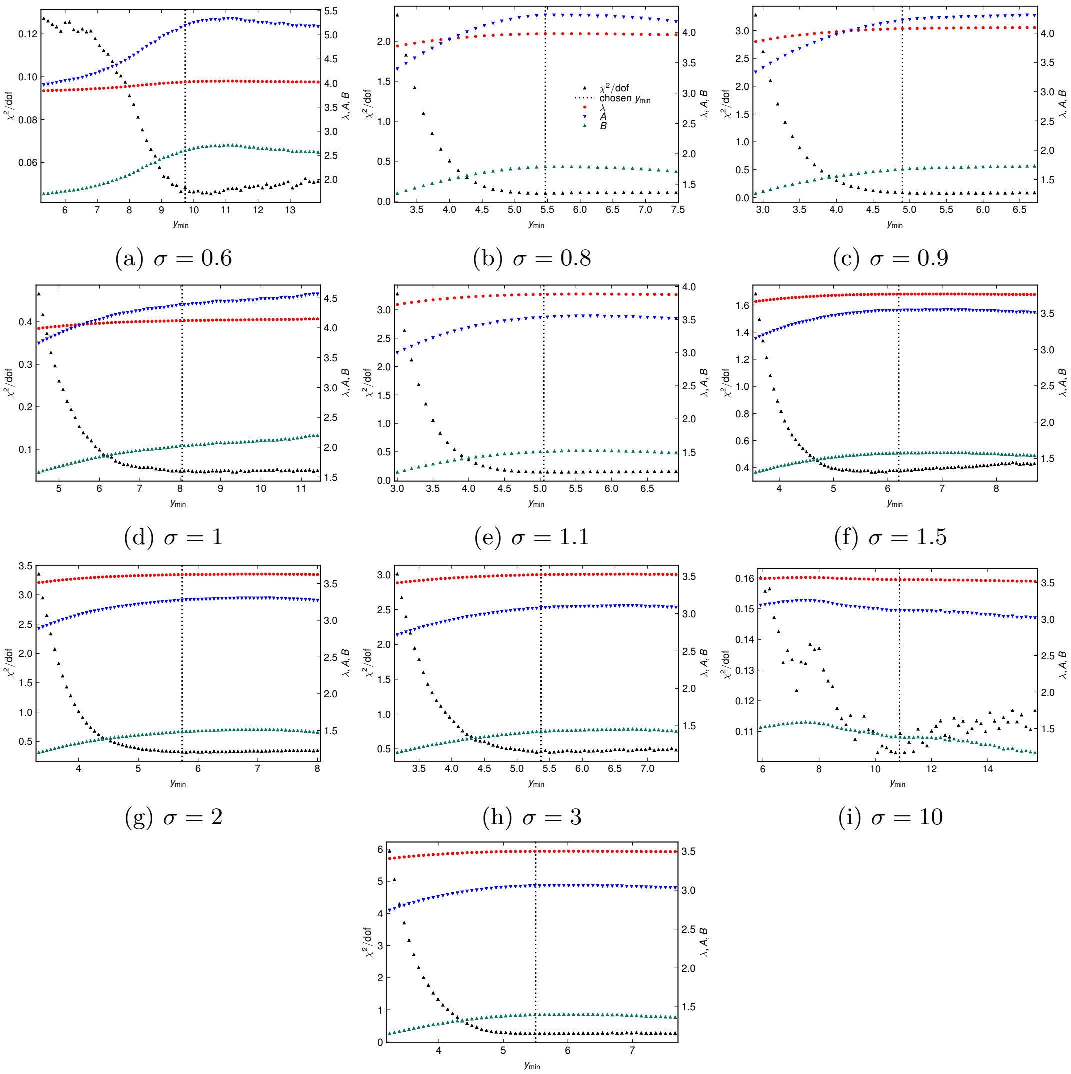

(a) $\sigma = 0.6$ (b) $\sigma = 0.8$ (c) $\sigma = 0.9$

(d) $\sigma = 1$ (e) $\sigma = 1.1$ (f) $\sigma = 1.5$

(g) $\sigma = 2$ (h) $\sigma = 3$ (i) $\sigma = 10$

(j) NN

FIG. S4: Same as Fig. S3 for the fit ansatz $f(y) = Ay^{-\lambda/z}(1 - B/y)$ with correction term.

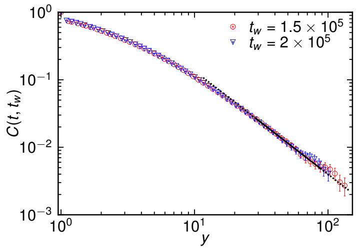

(a) $\sigma = 0.6,\ \lambda = 4.03 \pm 0.38$

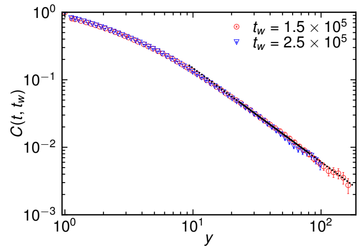

(b) $\sigma = 0.8,\ \lambda = 3.93 \pm 0.16$

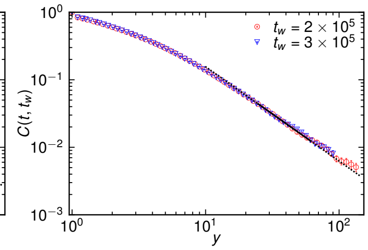

(c) $\sigma = 0.9,\ \lambda = 3.86 \pm 0.09$

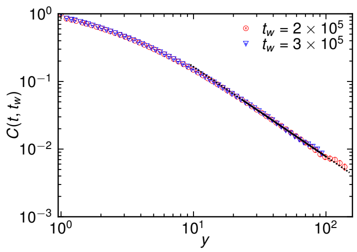

(d) $\sigma = 1,\ \lambda = 3.97 \pm 0.13$

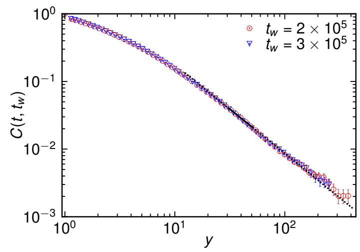

(e) $\sigma = 1.1,\ \lambda = 4.02 \pm 0.15$

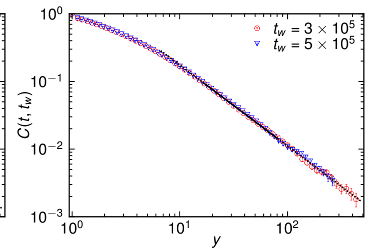

(f) $\sigma = 1.5,\ \lambda = 3.58 \pm 0.06$

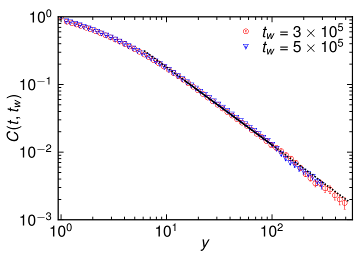

(g) $\sigma = 2,\ \lambda = 3.47 \pm 0.04$

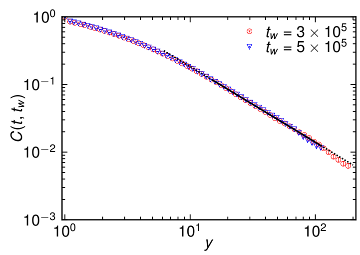

(h) $\sigma = 3,\ \lambda = 3.36 \pm 0.04$

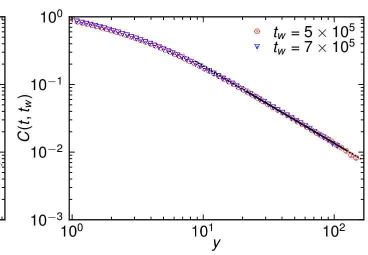

(i) $\sigma = 10,\ \lambda = 3.43 \pm 0.06$

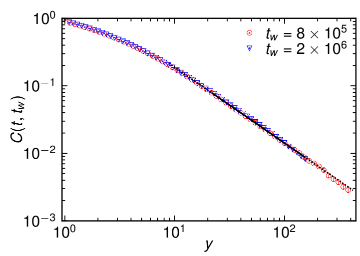

(j) NN, $\lambda = 3.45 \pm 0.08$

FIG. S5: Plots of the asymptotic fits $f(y) = Ay^{-\lambda/z}$ to $C(t, t_w)$ where the data for the smaller t_w are fitted in the previously chosen intervals $[y_{\min}, y_{\max}]$. The solid lines indicate the fitting range and the dotted lines represent the continuation of the fits beyond the fitting interval.

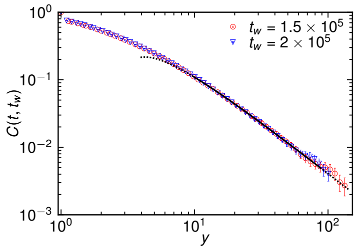

(a) $\sigma = 0.6,\ \lambda = 4.06 \pm 0.26$

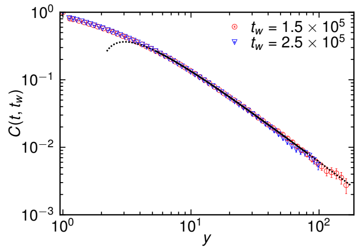

(b) $\sigma = 0.8,\ \lambda = 3.98 \pm 0.09$

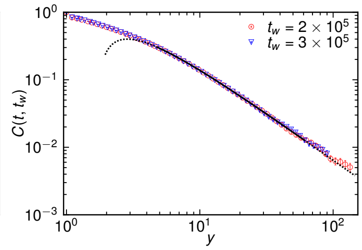

(c) $\sigma = 0.9,\ \lambda = 4.06 \pm 0.07$

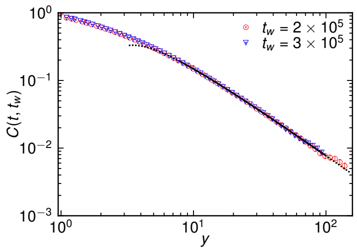

(d) $\sigma = 1,\ \lambda = 4.12 \pm 0.10$

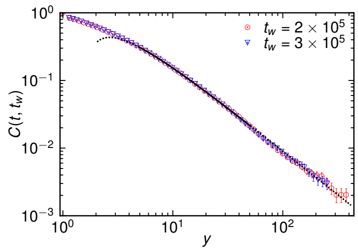

(e) $\sigma = 1.1,\ \lambda = 3.93 \pm 0.06$

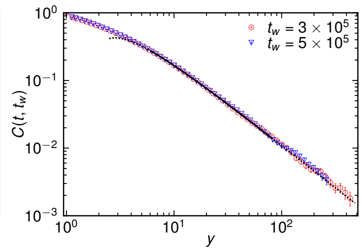

(f) $\sigma = 1.5,\ \lambda = 3.74 \pm 0.05$

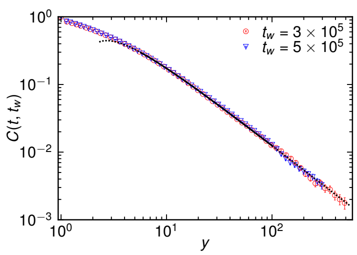

(g) $\sigma = 2,\ \lambda = 3.62 \pm 0.04$

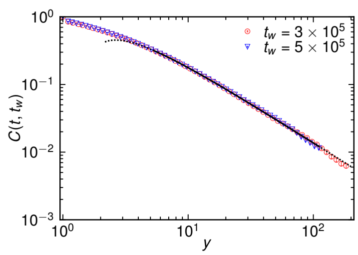

(h) $\sigma = 3,\ \lambda = 3.52 \pm 0.04$

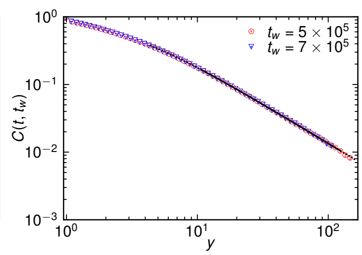

(i) $\sigma = 10,\ \lambda = 3.54 \pm 0.08$

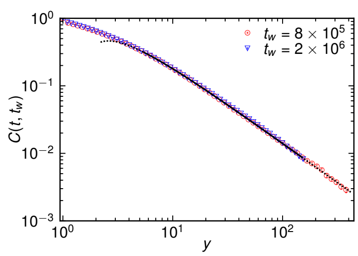

(j) NN, $\lambda = 3.50 \pm 0.03$

FIG. S6: Same as Fig. S5 for the fits $f(y) = Ay^{-\lambda/z}(1 - B/y)$ with correction term.

Table S1: Fit parameters for the asymptotic fit $f(y) = Ay^{-\lambda/z}$.

input								results		
L	σ	t_w	$t_{\min}$	$t_{\max}$	$\ell(t_w)$	$\ell(t_{\min})$	$\ell(t_{\max})$	χ^2/dof	λ	A
2048	0.6	1.50×10^5	4.35×10^6	1.32×10^7	60.2	200.1	304	0.04	4.03(39)	4.9(2.6)
2048	0.8	1.50×10^5	3.47×10^6	1.22×10^7	46.8	136.9	214	0.06	3.90(17)	3.70(74)
2048	0.9	2.00×10^5	4.96×10^6	1.22×10^7	46.2	137.9	191	0.11	4.04(18)	3.83(79)
2048	1	2.00×10^5	4.71×10^6	2.00×10^7	42.2	122.2	204	0.11	3.98(14)	3.49(55)
1024	1.1	2.00×10^5	6.15×10^6	1.02×10^7	38.9	121.8	145	0.03	3.93(17)	3.60(69)
1024	1.5	3.00×10^5	4.98×10^6	2.43×10^7	34.4	86.3	148	0.34	3.604(64)	2.79(19)
1024	2	3.00×10^5	4.59×10^6	3.03×10^7	28.3	68.4	129	0.08	3.455(42)	2.56(11)
512	3	3.00×10^5	4.61×10^6	3.33×10^7	23.3	55.7	109	0.21	3.357(45)	2.42(11)
512	10	5.00×10^5	1.09×10^7	6.25×10^7	20.6	55.7	101	0.09	3.431(59)	2.62(18)
1024	NN	8.00×10^5	1.76×10^7	1.21×10^8	20.4	56.0	108	0.09	3.367(39)	2.49(11)

Table S2: Fit parameters for the fit with correction $f(y) = Ay^{-\lambda/z}(1 - B/y)$.

input								results			
L	σ	t_w	$t_{\min}$	$t_{\max}$	$\ell(t_w)$	$\ell(t_{\min})$	$\ell(t_{\max})$	χ^2/dof	λ	A	B
2048	0.6	1.50×10^5	1.46×10^6	1.32×10^7	60.2	134.1	304	0.05	4.06(26)	5.5(1.9)	2.71(88)
2048	0.8	1.50×10^5	8.20×10^5	1.22×10^7	46.8	82.7	214	0.10	3.974(89)	4.26(41)	1.77(16)
2048	0.9	2.00×10^5	9.80×10^5	1.22×10^7	46.2	78.2	191	0.09	4.082(75)	4.24(30)	1.68(11)
2048	1	2.00×10^5	1.61×10^6	2.00×10^7	42.2	84.3	204	0.05	4.12(11)	4.42(53)	2.06(31)
1024	1.1	2.00×10^5	1.01×10^6	1.02×10^7	38.9	65.9	145	0.14	3.867(53)	3.49(18)	1.487(89)
1024	1.5	3.00×10^5	1.86×10^6	2.43×10^7	34.4	62.0	148	0.38	3.772(58)	3.58(23)	1.60(14)
1024	2	3.00×10^5	1.72×10^6	3.03×10^7	28.3	49.4	129	0.32	3.626(40)	3.29(14)	1.494(85)
512	3	3.00×10^5	1.61×10^6	3.33×10^7	23.3	39.4	109	0.45	3.518(41)	3.07(13)	1.424(83)
512	10	5.00×10^5	5.43×10^6	6.25×10^7	20.6	44.2	101	0.10	3.540(83)	3.12(34)	1.39(42)
1024	NN	8.00×10^5	4.40×10^6	1.21×10^8	20.4	35.2	108	0.26	3.500(26)	3.056(81)	1.399(54)

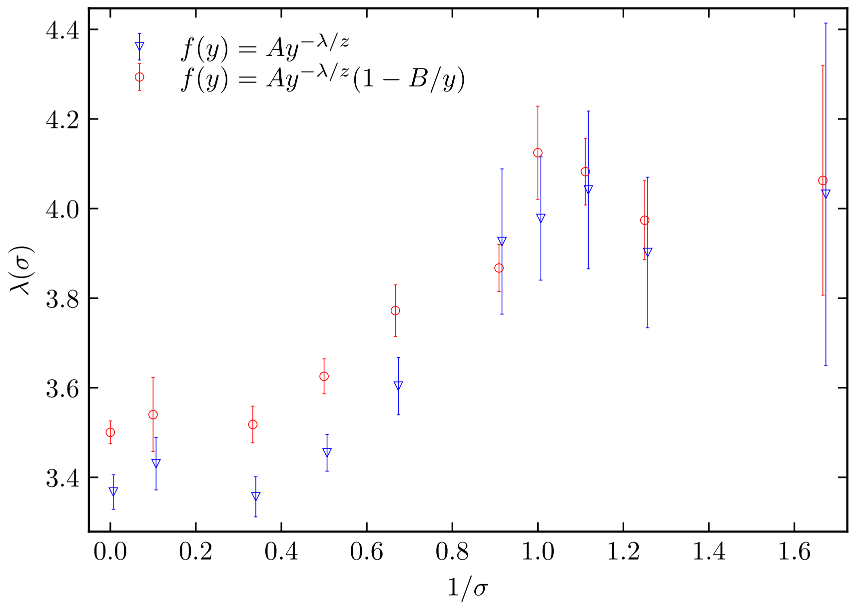

FIG. S7: Comparison of the σ-dependence of λ for the two considered fit ansätze.